[PROC. OF JSCE Structural Eng./Earthquake Eng. Vol. 2, No. 2 October 1985]

# ESTIMATION OF FATIGUE CRACK GROWTH BY ULTRASONIC IMAGING METHOD

*By Kenji SAKAMOTO*, Makoto FUKAZAWA**, Masayoshi HAMANO*** and Jiro TAJIMA*****

For a partially penetrated corner joint, estimations of the fatigue crack size and the crack growth behavior are investigated using the ultrasonic imaging method. Experimental results are obtained as follows :

1. An approximate estimation of the crack size is possible basing on its relation to the ultrasonic defect image.
2. The crack growth behavior can be estimated with reasonable accuracy from the increase of defect image size.

## 1. INTRODUCTION

The fatigue design of highway and railway combination type in the Honshu-Shikoku Bridges is based on the fracture control design, ensuring that fatigue cracks do not penetrate the full thickness within 100 years of the service life[1]. This design criterion is defined according to the results obtained from past fatigue tests on large scale specimens. These results show that fatigue cracks are formed at the early stage of repeated load, most of their fatigue lives to failure are spent on the propagation, and the concept of fracture mechanics is very valuable in order to classify the fatigue characteristics.

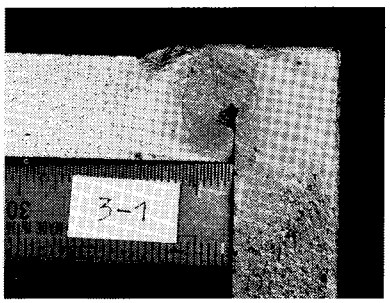


Photo 1 Fatigue crack originating from blowhole.

In case of the partially penetrated corner weld of a truss chord member, fatigue crack sometimes develops from a blowhole at the root (Photo 1). In order to prevent a fatigue failure originating from this weld defect, a partially penetrated groove weld is classified as Category B in the fatigue design specification (its design allowable stress range is $\sigma_{f0}=125$ MPa)[2]. Additionally, in the fabrication standard, members are classified according to their degree of importance, that is the ratio of the stress range acting on a member to allowable stress range, with the allowable defect size being defined for each class[3]. However, considering the possibilities of cracking from the allowable blowholes, as well as the

* Member of JSCE, Honshu-Shikoku Bridge Authority (Mori Bld. No. 22, Toranomon 4-3-20, Minato-Ku, Tokyo)
** Member of JSCE, Yokogawa Bridge Works (88 Shinminato, Chiba-Shi, Chiba)
*** Canon Sales Co., Inc, (11-28 Mita 3-Chome, Minato-Ku, Tokyo)
**** Member of JSCE, Dr. of Eng., Professor, Dept. of Construction Engineering, Saitama University (255 Shimookubo, Urawa-Shi, Saitama)

lack of accuracy of the non-destructive testing during fabrication, it must seem absolutely essential that periodic inspections of fatigue cracks and their spreading are carried out.

At present, non-destructive testing method to estimate the size of a fatigue crack originating at the blowhole at the root of partially penetrated groove weld has not been fully established. It is considered difficult to discover a fatigue crack originating at a blowhole with complicated three-dimensional figure. From the point of view of detecting fatigue cracks, it is necessary to develop an efficient inspection method covering a wide area. This method must be able to keep a record of cracks, which in turn will enable any spreading of cracks to be observed. In this study, the automatic ultrasonic image testing method was applied as a possible effective method.

The test procedure was as follows :

1) Possibility of estimation of the crack size is investigated by the correlation between the ultrasonic defect image and the actual fatigue crack using fatigue test specimens which have many concealed crack.
2) Availability of ultrasonic imaging method was investigated by measuring the crack size at preselected intervals of repeated loading cycles to trace its development using box-section specimen.
3) Considering the real structure, a truss model member was used for the purpose of tracing the development of the fatigue crack.

Finally, reliability and adaptability of this method are evaluated and some future problems are considered in this paper.

## 2. ULTRASONIC INSPECTION METHOD

At present, the peak echo method and the mode transfer surface wave method have been proposed as ultrasonic techniques for the purpose of estimating the depth of unexposed or exposed cracks[4]. Although these techniques are effective in the limit detection area or the known area of defects, no effective method or equipment has yet been developed for carrying out continuous detection in a large inspection area with the capability of recording defects. In this study, we consider the ultrasonic imaging method as an effective means for determining the presence of fatigue cracks, as well as their development and rate of growth during service life.

The system applied in this study is the Canon's automatic ultrasonic imaging system M 500-CHP-5. Fig. 1 shows the composition of its system, scanning position ($X$, $Y$) of probe, travel time and intensity of reflected signal are logically combined within imaging processing unit M-500 IP. The defect image is displayed in CRT monitor and is recorded on the continuous print paper with thermal dot printer using reflected signal above designated threshold level. The size of defect image was adopted as an estimation size of fatigue crack. The probe moves continuously in the direction which is at right angle

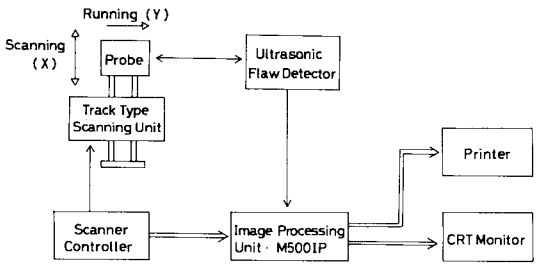


Fig. 1 System diagram.

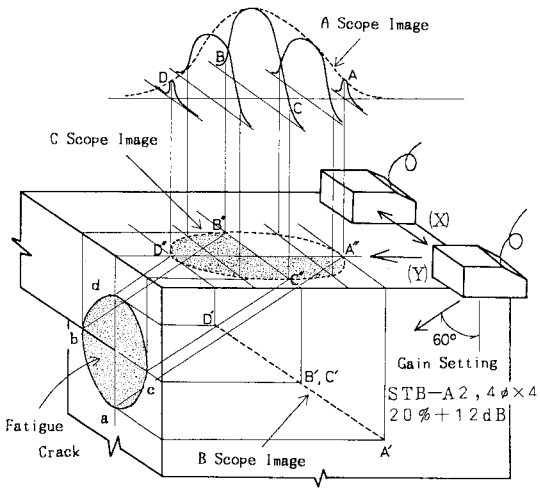


Fig. 2 Crack detection and drawing method.

to the root line of partially penetrated weld direction, and moves in steps parallel to the root line.

Fig. 2 shows the detection method and crack image drawing method used by automatic ultrasonic imaging system. Basic ultrasonic images are grouped into three types, A scope image, B scope image and C scope image. A scope image is a trend line of maximum echo height of echo scan line and B scope image is a sectional view perpendicular to the scanning direction obtained by calculating the travel time of reflected signal without angle correction. C scope image is a plane view in which the coordinates of defect signal above a threshold level are projected to a scanning plane and the incidence angle and shape is almost the same as that of actual fatigue crack. If both actual fatigue crack and defect image produced from the fatigue crack are geometrically equal, height $\overline{bc}$ of fatigue crack corresponds to $\overline{B''C''}$ of C scope image. Also, width $\overline{ab}$ of fatigue crack corresponds to $\overline{A''D''}\times\tan 30^\circ$ by incidence angle $60^\circ$ of shear wave. Therefore, the size of $\overline{B''C''}$ and $\overline{A''D''}\times\tan 30^\circ$ of defect image are adopted as an estimated size of fatigue crack.

The prove is contact focused shear wave type and has the following specifications :

Frequency : 5 MHz
Reflect angle : $60^\circ$
Diameter of probe : 15 mm$\phi$
Focal length : 20 mm
Minimum beam diameter of shear wave : 3.2 mm

As the size of defect image depends on the threshold level and reciever amplitude of ultrasonic flaw detector, we referred to the Japan Industrial Standard, Method of ultrasonic manual testing and classification of test results for ferritic welds, JIS Z 3060-1983. Gain setting was made in such a way that the echo height of a 4 mm $\phi\times$4 mm calibration hole of STB-A 2 standard test block was 80 % and the return signal above 20 % threshold level in vertical monitor scale of A scope was recorded. This detection level is equivalent to L-line detection level of JIS Z 3060.

## 3. SIZE ESTIMATION OF CONCEALED FATIGUE CRACK

Possibility of the size estimation by the ultrasonic imaging method regarding the fatigue crack originating at the root blowhole in the corner weld was investigated. Specimens are of a box section type tested for another purpose[5]. Maximum stress range is 173 MPa. Ultrasonic testing was conducted in the horizontal position under no load. Then, the corner weld was destroyed along the weld root to expose the fatigue crack as shown in Fig. 3 and correlation between the fatigue crack size and ultrasonic defect image size was considered.

Fig. 4 shows the typical ultrasonic defect images of fatigue cracks. Fatigue test of this sample was finished at $136\times10^4$ cycles and ultrasonic testing was conducted two times, $100\times10^4$ cycles and after fatigue test, so that the ultrasonic images of fatigue cracks at the two different cycles were shown. Normal beam ultrasonic inspection was carried out to detect the root blowhole at fabrication. Two circular fatigue cracks of about 10 mm in diameter developed at the root blowhole and almost identical crack images of the ultrasonic testing were also recorded as actual fatigue cracks. On the other hand, the defect image of comparatively large size produced by the blowholes itself was recorded and it is not possible to determine the cause of the fatigue cracks. Nevertheless, it seems possible to determine the crack development from the extension of B scope image. In addition, the

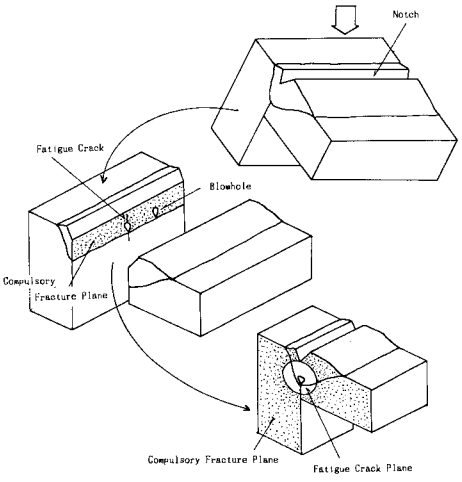


Fig. 3 Fatigue crack exposure method.

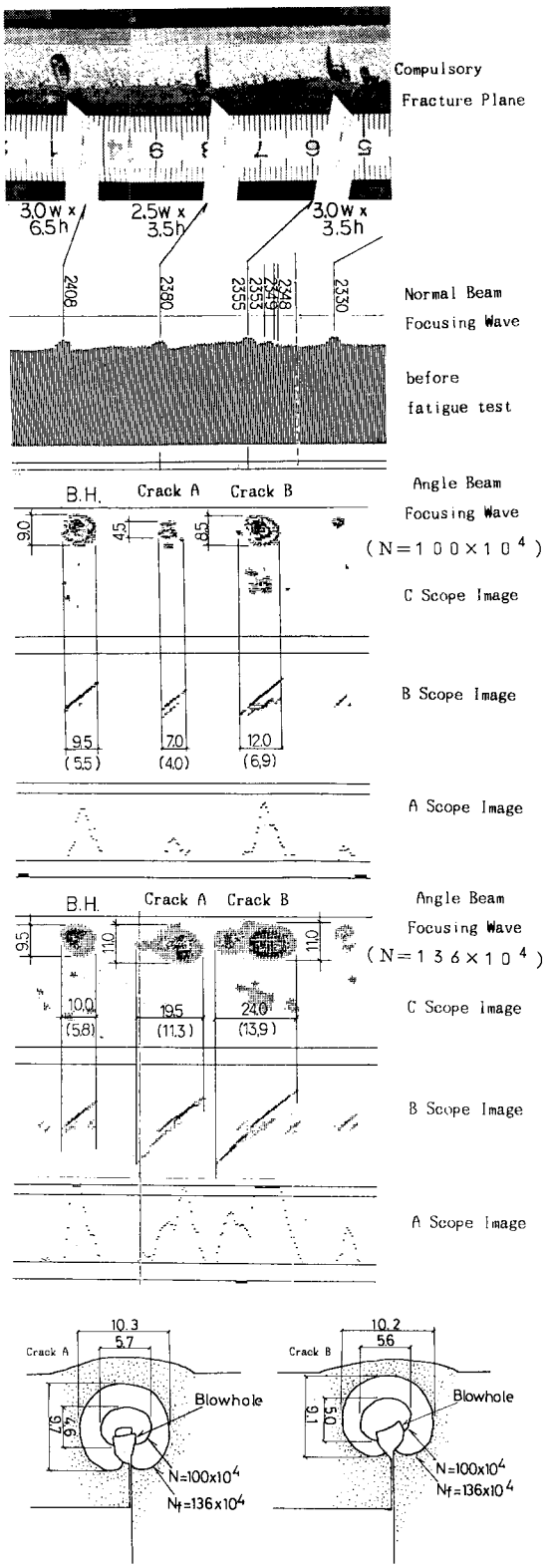


Fig. 4 Typical ulrasonic images of fatigue eracks.

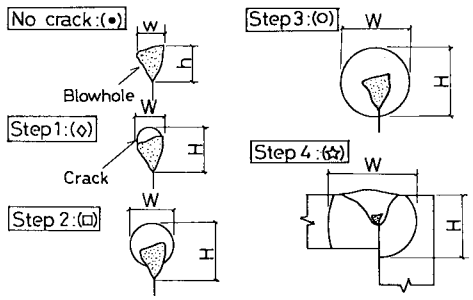


Fig. 5 Process of crack growth.

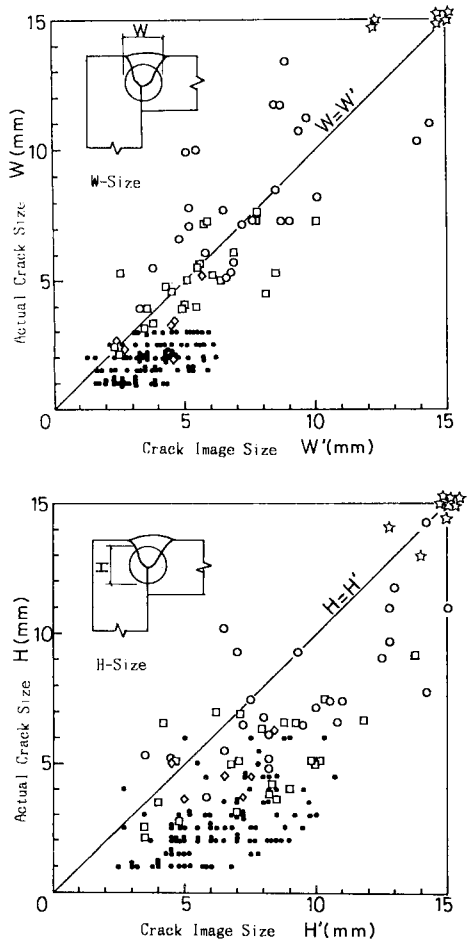


Fig. 6 Relation between crack size and image size.

defect images of blowholes only are almost the same size, but the defect image of fatigue crack becomes larger with an increase of loading cycles comparing two images at 100 $\times 10^4$ and 136$\times 10^4$ cycles.

In this investigation, there were about sixty fatigue cracks of various sizes. Each fatigue crack originated from the top of the blowhole and spread in a circular shape. The fatigue cracks were classified by the step of crack growth as shown in Fig. 5. The size of blowhole is represented by width $w$, and height $h$, and the size of fatigue crack was defined by $W$ and $H$.

Fig. 6 shows the relationship between fatigue crack and ultrasonic defect image according to each size of $W$ and $H$. The black mark is a blowhole which does not generate a fatigue crack, and cracks are classified by the marks shown in Fig. 5 which signify the stages of crack growth.

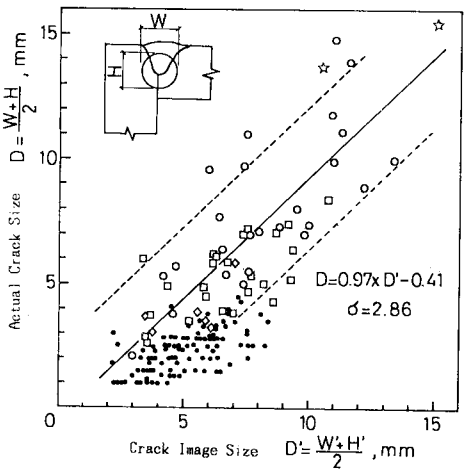


Fig. 7 Relation between crack size and image size.

These relationships show that the ultrasonic defect image size gets larger as the fatigue crack grows. With some dispersal, the relationship of the crack image is equivalent to the actual crack with regard to $W$ size, but the image has a tendency to become larger than the actual crack size with regard to $H$ size.

In case of circular shape of the fatigue crack with a diameter of $D=(W+H)/2$, test results on the relationship between actual crack and ultrasonic image are also shown in Fig. 7. As the regression line has a gradient of almost 1.0, the size of ultrasonic image is equal to the actual crack size but the standard deviation is 3 mm. In this figure, the images of blowholes, size of which is $w \leqq 3$ mm and $h \leqq 6$ mm, are plotted. It shows that the blowhole was recorded as relatively large defect images, so that the crack development at the early stage cannot be decided by this relationship alone. And the test data do not show any significant difference in the correlation among the stages of crack growth.

Considering above mentioned relationships, ultrasonic imaging method gives a possibility to estimate the crack size with some dispersal. Additionally, a comparison of the ultrasonic images at each stage of repeated loading cycles is considered useful for the evaluation of the crack development. In the following section, the possibility of tracing the growth of fatigue crack is considered, in addition to the estimation of the crack size by the two type box-section specimens tested with 4 MN fatigue testing machine.

## 4. TRACE OF FATIGUE CRACK DEVELOPMENT IN BOX-SECTION SPECIMEN

The surver was made to trace fatigue cracks developing from blowholes at roots by carrying out a fatigue test on a specimen of axis-tension type with box sectional area. Fig. 8 shows the configuration of the specimen. The specimen has a box sectional area of 300 mm$\times$130 mm in external dimensions and two weld lines, J 1 and J 2, with artificial blowholes at four positions, ① to ④, respectively. The artificial

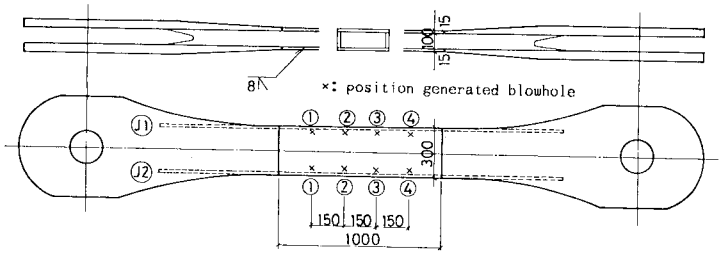


Fig. 8 Configuration and dimension of specimen.

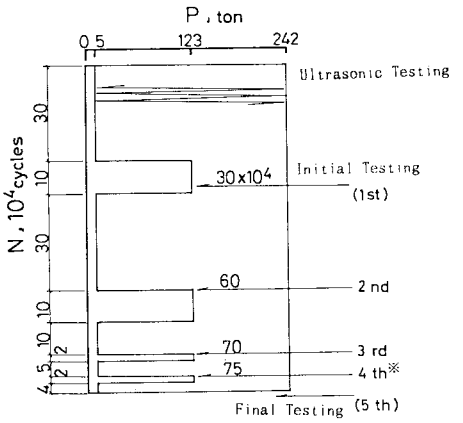


※ Crack of J1-2 penetrated through thickness

Fig. 9 History of fatigue test.

Photo 2 Ultrasonic testing condition.

blowholes have been provided by applying zinc-based paint on the surface of the roots. Fig. 9 shows the history of loading cycles and the time when ultrasonic testing was carried out. The range of test stress was 196 MPa and the test specimen was broken when loads were applied 79 $\times 10^4$ times. Ultrasonic testing was carried out five times and beachmarks with a half stress range were left before or after ultrasonic testing in order to check the crack size afterwards.

Ultrasonic testing was carried out on test specimen set in a testing device in vertical position under static tensile load of 153 MPa. Photo 2 shows the testing condition. The fatigue test was completed with remarkable growth of cracks developing from blowholes of J 1-②. Photo 3 shows the fracture surface of a fatigue crack and the result of beachmarks observation. It was observed that the crack originated from the side walls of blowhole large enough to reach surface. It could also be confirmed that

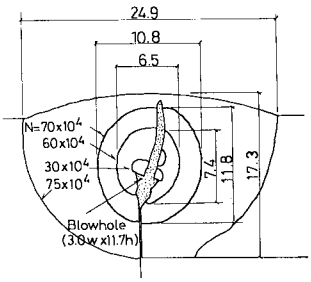


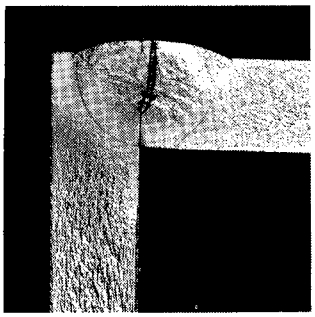

Photo 3 Fracture surface of crack (J 1-②).

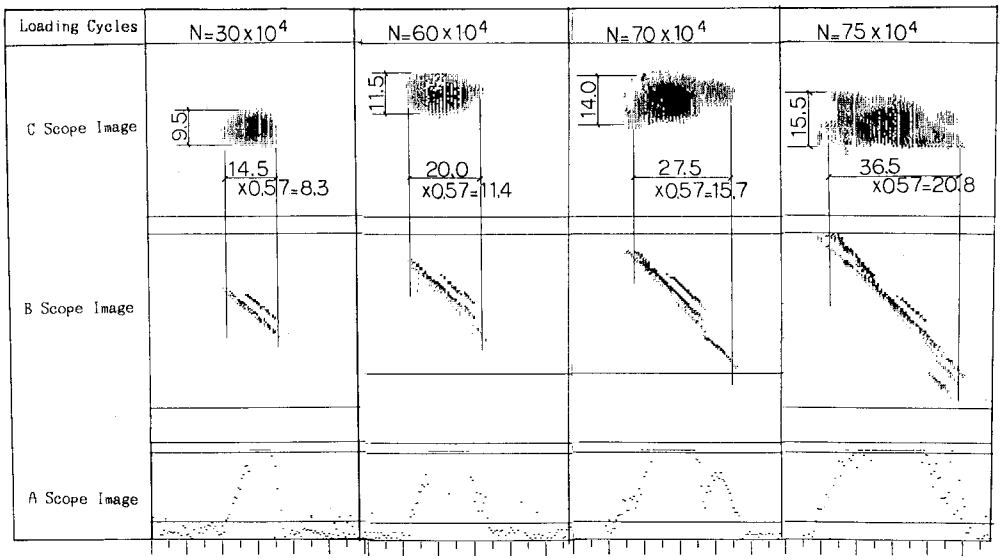


Fig. 10 Ultrasonic images of crack (J 1-②).

cracks had originated in the seven locations where the blowholes have been provided purposely.

The spreading of cracks could be observed for all cracks at eight locations by ultrasonic testing carried out in the course of the test. Cracks developed into final fracture, as can be seen from Fig. 10 and from the result of ultrasonic testing made on J 1-②. Crack image becomes larger as number of repeated cycles increases. This can be observed especially on the screan of B scope.

Fig. 11 shows the plotted relationship between the size of crack image at each detection and corresponding crack size (or beachmark size). A comparatively close correlation is observed with less dispersal as compared with the previous test result. The relationship between the two is obtained as follows, using the method of least squares.

$$D=0.98\,D'-3.0 \quad \cdots\cdots (1)$$

Standard deviation $=1.87$

Correlative coefficient $=0.86$

As seen in the above, the crack image size shows a tendency to increase by about 3 mm as compared with that of actual crack size. As ultrasonic testing was made under tensile load condition, it may be considered that echo from the plane of crack became larger due to the cracks being in open conditions. Further study is required on this point.

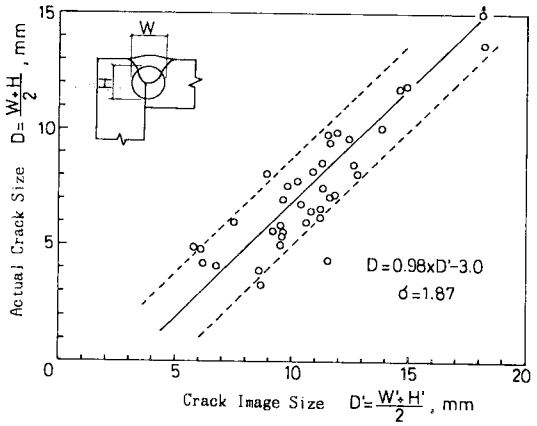


Fig. 11 Relation between crack size and image size.

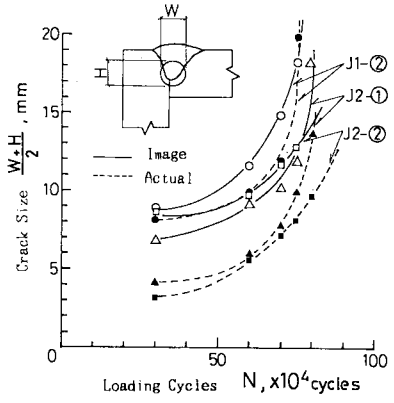


Fig. 12 Development of crack and ultrasonic image.

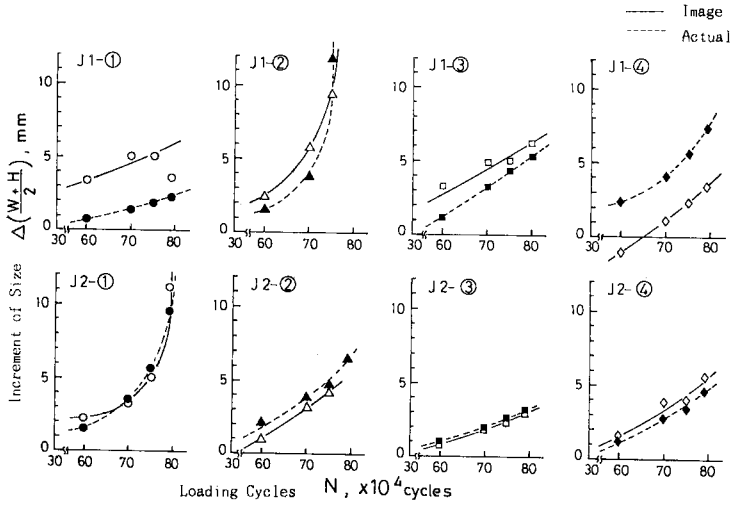


Fig. 13 Ordered arrangement of variations in crack size and crack image size.

Fig. 12 shows variation in crack size and crack image size due to repeated cycles for three representative cracks. The crack image size was larger than the actual crack size, but it was seen that it showed a tendency to increase in size as the crack developed. Fig. 13 shows an ordered arrangement of variations in the crack size and crack image size from the initial testing at the repeated cycles of $30\times10^4$. Except for J 1-① and J 1-④, the variation in the former corresponds well with that of the latter. For J 1-① and J 1-④, the crack image is shifted, either upon or down in relation to the actual cracks. It is considered that this was caused by error in setting of fundamental sensitivity as well as due to defective couplings. The ordered arrangement of variations from the repeated cycles of $60\times10^4$ shows considerable conformity between the two.

From the results, as aforesaid, it can be seen that the development of the cracks can be accurately understood if the data is orderly arranged by the variation in the crack images. However, attention must be directed to the fundamental sensitivity and defective couplings when ultrasonic testing is carried out.

## 5. TRACE OF FATIGUE CRACK DEVELOPMENT IN TRUSS PANEL-POINTED SPECIMEN

In order to pursue the fatigue crack growth originating at the corner weld, fatigue test of truss chord structure as a model of a stiffening truss member was investigated.

Fig. 14 shows the truss panel-point loading apparatus. The central part of lower chord is an object to be tested and Fig. 15 shows the precise details. There exist random blowholes at the root of corner weld.

Fig. 16 shows the history of loading cycles and the time of ultrasonic testing. At the first time, fatigue test was conducted with load range of 280 tons but

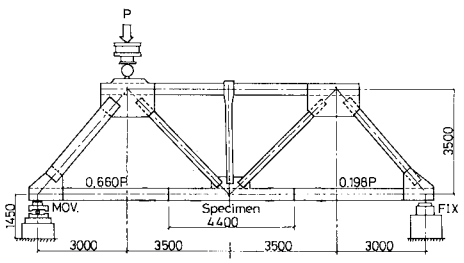


Fig. 14 Truss type loading apparatus.

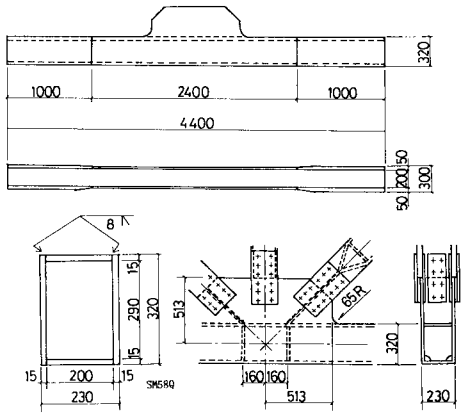


Fig. 15 Configuration and dimension of specimen.

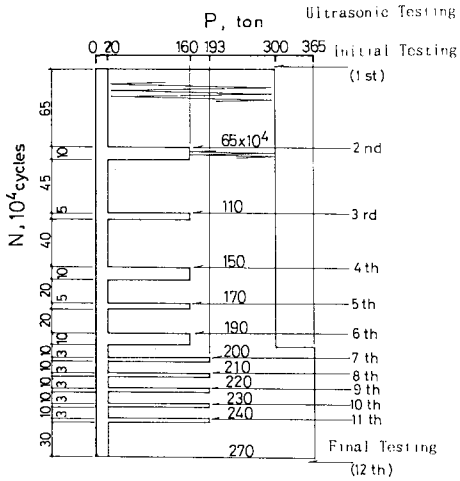


Fig. 16 History of fatigue test.

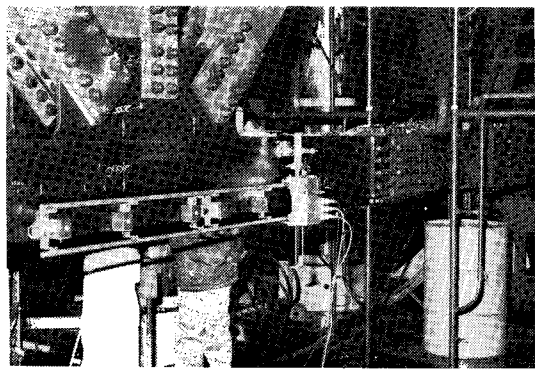

Photo 4 Ultrasonic testing condition.

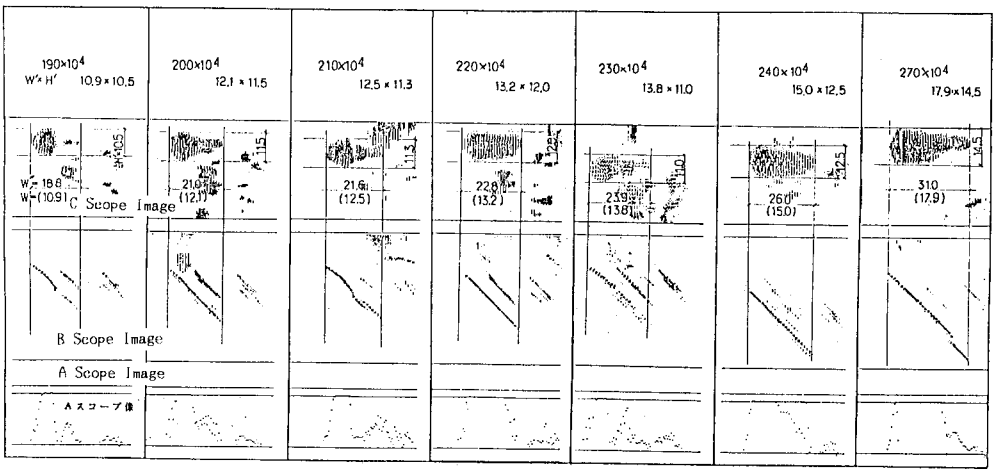


Fig. 17 Ultrasonic images of crack (3-1).

large growth of fatigue cracks could not be observed at $190\times10^4$ cycles. So, load was increased to 345 tons after these cycles.

Ultrasonic testing was conducted in a static loading condition of 20 tons which is equivalent to the lower load. After each testing, beach mark control was carried out with a half stress range. The calculation stress of lower chord with loading range of 280 tons is 116 MPa.

Photo 4 shows the ultrasonic testing condition. Testing was carried out in the moving position where axis force was large and testing position was the same as on the actual bridge. Moreover, tapered section was not tested because of the lack of scanner apparatus before $190\times10^4$ cycles. But considering the actual bridge with the same details this point was tested with usage of an adequate apparatus after $190\times10^4$ cycles. In the test, we could estimate that the crack in the corner weld of tapered section was growing comparatively rapidly.

Fig. 17 shows the result of ultrasonic testing of the crack, 3-1, originating from tapered section at each stage of load cycles. As the size of $D'=(W'+H')/2$ is 16.2 mm at $270\times10^4$ cycles, diameter of crack is expected to be 12.9 mm using equation (1) and also to increase by 5.5 mm compared with its diameter at $190\times10^4$ cycles. In the other part, another five cracks were found in the pursuit of ultrasonic testing.

Although the crack did not reach to the surface at $270\times10^4$ cycles, fatigue test was finished and crack investigation was carried out as shown in Fig. 3.

There were six cracks generated from the blowholes at the root of the corner weld. These cracks were already expected in the ultrasonic testing. Photo 5 shows the typical examples of crack surfaces and those beachmark observations. But as the cycles of beachmark were small, beachmark at $190\times10^4$ cycles only was obviously confirmed in the fracture surface.

In the two cracks, the variation of actual crack size and ultrasonic image size due to increase of load cycles was plotted in Fig. 18. The characteristic of Fig. 18 are very similar to box section type specimen. Trend line of ultrasonic crack image is shifted above that of actual crack size in

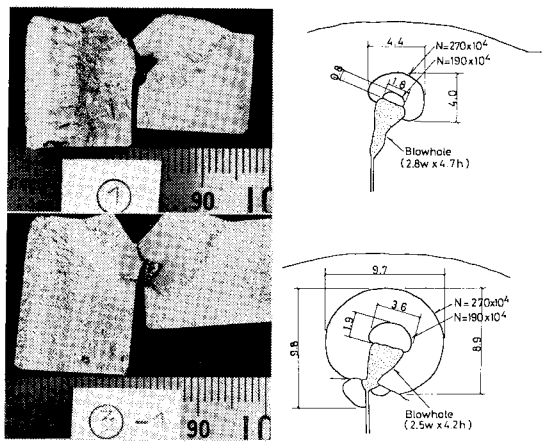


Photo 5 Appearance of typical cracks.

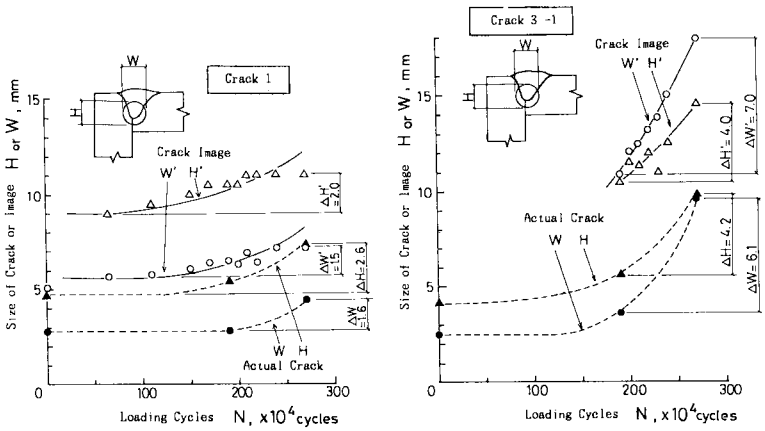


Fig. 18 Development of crack and ultrasonic image.

a load cycle and both degrees of size increase are also similar. When the extent of the size increase of crack image is calculated using image size before fatigue test and $190\times10^4$ cycles as an initial number, size of crack image almost corresponds with that of actual crack.

Fig. 19 shows the relaionship between the variation in the actual crack sizes and the crack image sizes, including the test result of the box-section specimen. As an initial value, the size at the repeated cycles of $190\times10^4$, when the cracks grew remarkably, was adopted for the truss panel-pointed specimen, and the size at the repeated cycles of $30\times10^4$ (in the initial testing) was adopted for the box section specimen. In all cases, it is observed that the variations are distributed on both sides of the following line and represent close correlation between the two.

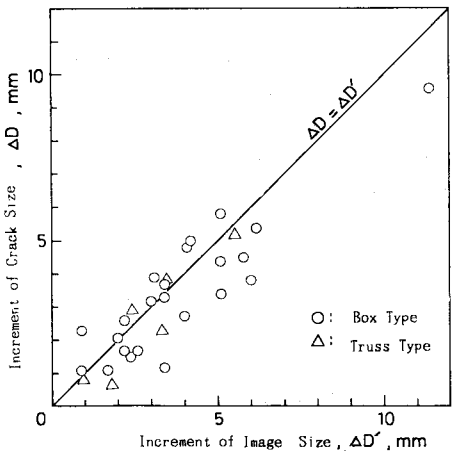


Fig. 19 Relation between variation in crack size and crack image size.

$$\Delta D=\Delta D' \quad \cdots\cdots (2)$$

It is possible to assume the behavior of the crack development by the evaluation of variations in the crack image size.

## 6. SUMMARY

For a partially penetrated corner joint, estimations of the fatigue crack size and the crack growth behavior are investigated using the ultrasonic imaging method. The test results are summarized as follows :

( 1 ) The relationship between the crack size, $D=(W+H)/2$ and the crack image size $D'=(W'+H')/2$ is represented by the following equation.

$D\fallingdotseq D'-\alpha$

However, the value of $\alpha$ varies in a series of tests. Further study is therefore required, including the influence of applied stress conditions when crack detection is carried out.

( 2 ) When a crack is small, it is difficult to distinguish it from a blowhole. However, when it grows larger, it can be identified as a crack in the image on the screen of B scope.

( 3 ) The relationship between the variation, $\Delta D$ in crack size and that in the crack image size, $\Delta D'$ is expressed as follows.

$\Delta D = \Delta D'$

Therefore, the development of a crack can be estimated basing on the variation of the crack image in flaw detection after a certain number of repeated cycles.

The automatic ultrasonic flaw detecting system introduced in this paper may be an effective means for crack detection by taking into consideration rough crack detection over a wide area on structual members, and combining with a precision inspection on the area where the existence of cracks is confirmed. The peak echo method is considered to be an effective means in this case. There are problems, however, in recognizing the echos from blowholes of complicated shape, those from the corners of cracks and the sources of cracks.

When stiffening truss chord members are the objects of tests, further study will be carried out on thick and painted members on large-scale fatigue specimens.

## ACKNOWLEDGEMENT

In closing, we wish to express our sincere appreciation for the cooperatoin and assistance extended to us by all the staff of the Construction Equipment Mecnanization Research Institute where the large-scale fatigue tests were carried out. We wish also to take advantage of this occasion by expressing our appreciation to the members of the Ocean Bridge Construction Research Institute and the Study Committee for nondestructive inspection method for their valuable suggestions, discussions and advice on this study.

REFERENCES

1) Japan Sociaty of Civil Engineers, Report on the Steel Superstructure of Honshu-Shikoku Bridges, 1981 (In Japanese).
2) Japan Sociaty of Civil Engineers, Report on the Steel Superstructure of Honshu-Shikoku Bridges, 1983 (In Japanese).
3) Kubomura, K., Shimokawa, H. and Takena, K. : Technological Development of long-Spanned Bridges for Railway, Journal of the JSCE, Vol. 68, No. 7, 1983.
4) Proposed Japan Industrial Standard : Measuring Methods of Shape and Size of Defects in Steel Welds using Ultrasonic Test Methods, Report of NDI, 1985 (In Japanese).
5) Fukazawa, M., Natori, T., Terada, H., and Akashi, S. : Effect of Stress Relief on Fatigue Strength of High Strength Steel Corner Joint with Blowhole, Proc, of JSCE, No. 356, 1985. 4.

(Received May 28 1985)